Current Drug Metabolism, 2020, *21*, 357-367

RESEARCH ARTICLE

Absorption, Metabolism and Excretion of Surufatinib in Rats and Humans

Ke Li[1], Sheng Ma[2,5], Liyan Miao[2,5,*], Songhua Fan[1], Bin Pan[1], Weihan Zhang[1], Weiguo Su[1], Yating Xiong[3], Zheming Gu[3], Lian Guo[4] and Yang Sai[1,*]

[1]*Hutchison MediPharma Ltd., Shanghai, China;* [2]*The First Affiliated Hospital of Soochow University, Suzhou, China;* [3]*Jiangsu Value Pharmaceutical Services Co., Ltd., Nanjing, China;* [4]*XBL-China, Inc., Nanjing, China;* [5]*Institute for Interdisciplinary Drug Research and Translational Sciences, College of Pharmaceutical Sciences, Soochow University, Suzhou, China*

ARTICLE HISTORY

Received: December 10, 2019
Revised: March 13, 2020
Accepted: April 08, 2020

DOI:
10.2174/1389200221666200514131721

Abstract: ***Background*:** Surufatinib is a potent small-molecule tyrosine kinase inhibitor and exhibited significant efficacy in the treatment of neuroendocrine tumors in clinical trials.

***Objective*:** The absorption, metabolism and excretion of surufatinib were investigated in rats and human volunteers following a single oral dose of [^{14}C] surufatinib.

***Methods*:** The radioactivity was measured in plasma, urine, feces and bile by liquid scintillation counting, and the metabolites were characterized by liquid chromatography coupled to mass spectrometry.

***Results*:** Surufatinib was orally absorbed similarly in rats and human volunteers, with the median T_{max} of 4 hours post-dose. The estimated $t_{1/2}$ appeared longer in humans than in rats (mean $t_{1/2}$: 3.12 hour for male rats, 6.48 hours for female rats and 23.3 hours for male human volunteers). The excretion of surufatinib was almost complete in rats and human volunteers in the studies, with the total radioactivity recovery of >90% of the dose. Similarly, in rats and humans, fecal excretion predominated (approximately 87% of the dose recovered in feces and only 5% in urine). The parent drug was the major radioactive component detected in the plasma extracts of rats and humans, and no single circulating metabolite accounted for >10% of the total radioactivity. Unchanged drug was a minor radioactive component in the excreta of rats and humans.

***Conclusion*:** Fecal excretion was the predominant way for the elimination of surufatinib and its metabolites in rats and humans. No disproportionate circulating metabolite was observed in humans.

Keywords: Anticancer drug, pharmacokinetics, absorption, excretion, metabolism, surufatinib.

1. INTRODUCTION

Neuroendocrine tumors (NETs) are rare neoplasms arising from diffusive neuroendocrine cells of various organs. In the past four decades, the age-adjusted incidence rate increased 6.4-fold in the United States, from 1.09 per 100,000 persons in 1973 to 6.98 per 100,000 persons in 2012 [1]. In China, a similar trend was identified by a hospital-based, nationwide, retrospective epidemiological study of gastroenteropancreatic neuroendocrine neoplasms [2]. Treatment options for advanced, low or intermediate grade NETs include somatostatin receptor-targeting therapeutics, peptide receptor radionuclide therapy, systemic chemotherapies, targeted agents, and local-regional treatments [3]. Nearly half of all patients with NETs have distant metastasis at initial diagnosis [3]. The median survival time for patients with well-differentiated to a moderately differentiated distant stage of NETs varied by tumor origins, approximately 14 months for colonic origin, 60 months for the pancreatic origin and 103 months for small intestine origin [1]. Although NETs are highly vascularized neoplasms, those originating from diverse organs respond to anti-angiogenesis treatment differently [4-6]. In phase III pivotal study, sunitinib significantly prolonged progression-free survival (PFS) in patients with pancreatic NETs compared with placebo but failed to demonstrate efficacy in extrapancreatic NETs. Fibroblast growth factor (FGF) 2 was shown to be a potent mediator in anti-angiogenesis resistance development, and inhibiting FGF receptor signaling could overcome resistance [7]. Preclinical cancer models also showed that macrophages, usually recruited and activated by colony-stimulating factor 1 receptor (CSF-1R), played a pro-angiogenic role in the tumor microenvironment. Furthermore, eliminating tumor-associated macrophages by inhibiting CSF-1R led to decreased neoangiogenesis [8]. Therefore, inhibiting these targets simultaneously could be a promising anti-angiogenic strategy.

Surufatinib is a potent small-molecule tyrosine kinase inhibitor (TKI), selectively targeting vascular endothelial growth factor receptors (VEGFR) 1, 2, and 3, fibroblast growth factor receptor (FGFR) 1 and CSF-1R. In the phase I dose-finding study in patients with advanced solid tumors, surufatinib demonstrated anti-tumor activities in patients with NETs [9]. The efficacy and safety of surufatinib in patients with pancreatic or extra-pancreatic NETs were further evaluated in a phase II trial, which showed encouraging anti-tumor activities and manageable toxicities [10]. In a phase III study of surufatinib or placebo on patients with well-differentiated, progressive, unresectable or metastatic extrapancreatic NETs (NCT02588170, results presented at 2019 European Society for Medical Oncology Congress), the study met the primary endpoint of disease progression-free survival (PFS). Currently, another phase III study is underway for the validation of the efficacy in patients with pancreatic NETs.

Assessment of absorption, metabolism and excretion (AME) of a drug candidate in humans with radiolabeled material, known as human mass balance study, is critical in providing information

*Address correspondence to these authors at the Building 4, 720 Cailun Road, Shanghai, China; Tel: 86-21-20673030; E-mail: yangs@hmplglobal.com
899 Pinghai Road, Suzhou, China; Tel: 86-512-67972998;
E-mail: miaolysuzhou@163.com

 © 2020 Bentham Science Publishers

Current Drug Metabolism

about systemic circulating metabolites that may pose safety concerns due to the formation of human disproportionate metabolites. The circulating metabolites in humans need to be adequately exposed to the animal species used in toxicology studies [11]. The extent of excretion and elimination pathways for the parent drug and metabolites investigated in the AME studies help to guide further clinical pharmacology research such as drug-drug interaction studies and pharmacokinetic studies in the patients with impaired elimination functions [12,13]. Furthermore, the knowledge of elimination pathways may trigger the investigation of drug transporters involved in the excretion of drugs and metabolites *via* the kidneys or the liver [13]. The present study characterized the AME of surufatinib in humans and rats, and this is the first disclosure of the study results.

2. MATERIALS AND METHODS

2.1. Chemicals and Reagents

Surufatinib (chemical purity > 98%), [^{14}C] surufatinib (57.6 mCi/mmol, chemical purity: 99.2%, radiochemical purity: 99.4%) and the reference compound HM5013621 (M18) were provided by Hutchison MediPharma Ltd (Shanghai, China). Ultima Gold Scintillation Liquid was purchased from PerkinElmer (Downers Grove, IL, US). Ammonium acetate was ordered from Sigma-Aldrich (St. Louis, MO, US). Acetonitrile, methanol, and other organic solvents were purchased from Merck (Kenilworth, NJ, US). Water was prepared in-house using a Millipore Water Purification System (Bedford, MA, US).

2.2. AME Study in Rats

The AME study in rats was conducted at XBL-China, Inc. (Nanjing, China). The study protocol was reviewed and approved by XBL-China's Institutional Animal Care and Use Committee (IACUC). Sprague-Dawley rats were purchased from Vital River Laboratories (Beijing, China) with the age of 8 ~ 12 weeks and weight of 199 –256 g. Bile duct cannulated (BDC) rats were prepared 3 to 5 days before the dosing days by performing surgery of indwelling a bile duct cannula in each rat. Rats had access to food and water *ad libitum* during the study except for fasting overnight prior to dosing and withdrawal of food until 4 hours post-dose. After a single oral dose of 40 mg/100 μCi/kg of [^{14}C] surufatinib (a suspension formulated in 0.5% carboxymethyl cellulose) in rats, urine, feces, cage rinse and carcass were collected up to 120 hours post-dose from intact rats (2 males and 2 females), and bile, urine, feces and cage rinse collected up to 72 hours post-dose from BDC rats (2 males and 2 females). Plasma samples were collected from jugular vein cannulated rats (3 males and 3 females) at 0.25, 0.5, 1, 2, 4, 8, 12, 24 and 48 h post-dose and from another group of intact rats (5 males and 5 females) at 2, 4, 8, 12 and 24 hours post-dose (1 male and 1 female sacrificed at each time point to collect sufficient plasma for metabolite identification). One rat was administered the formulation vehicle, and the samples of plasma, urine, feces and carcass were collected as negative controls. All the samples were stored at approximately -20^{o}C until sample analysis.

2.3. AME study in humans

This study was an open-label, single-center, single-dose study and approved by the ethical committee at the First Affiliated Hospital of Soochow University (Suzhou, China). Volunteer enrolment, drug administration and sample collection were performed by the First Affiliated Hospital of Soochow University, and formulation preparation and sample analysis were conducted at Value Pharmaceutical Services Co., Ltd. (Nanjing, China). Six healthy male volunteers with informed consent were enrolled in this study. The average age for the six volunteers was 29 years, and the mean body weight was 64 kg. Subjects were nonsmokers, with no history of drug or alcohol abuse and with no prescribed or non-prescribed medication within 14 days prior to the study commencing. Each of six volunteers was administered a single oral dose of 300 mg surufatinib containing 100 μCi [^{14}C] surufatinib (a suspension mainly formulated in microcrystalline cellulose) within 1 hour after having breakfast. To determine the exact amount of drug given to the volunteers, the suspension in each dosing bottle was measured after dose administration for any residual radioactivity. The volunteers were prohibited from drinking water for 1 h and fasted for 4 h after dosing. The dosimetry calculation was performed by Value Pharmaceutical Services Co., Ltd. to evaluate the absorbed radiation in individual organs and the effective dose (total body), using the data from a quantitative whole-body autoradiography study in male Long-Evans rats and a mass balance study in male Sprague-Dawley rats. Oral administration of 100 μCi [^{14}C] surufatinib was calculated to result in a total radiation burden of 0.26 mSv, categorized as a category IIa project (a minor level of risk, covering doses to the public from controlled sources) (International Commission on Radiologic Protection, 1991). Plasma samples were collected at pre-dose (0 hour) and at 0.5, 1, 2, 4, 6, 8, 12, 24, 36, 48, 72, 96, 120, 168 and 216 hours post-dose. Urine samples were collected at pre-dose (within 24 hours prior to drug administration), and at the following intervals of 0 to 4, 4 to 8, 8 to 12, 12 to 24 hours and then every 24 hours until 264 hours post-dose. Feces samples were collected at pre-dose (within 24 hours prior to drug administration) and every 24 hours up to 264 hours post-dose. Weights of urine and feces for each collection interval were recorded. The samples were stored at -20^{o}C until analysis.

The occurrence of adverse events (AEs) was monitored throughout the study. Safety was assessed by physical examinations, vital signs, clinical laboratory tests, 12-lead ECGs, and monitoring for adverse events (AEs) throughout the study. AEs were evaluated according to National Cancer Institute Common Terminology Criteria for Adverse Events (version 4.03) and were managed and recorded promptly by qualified investigators according to relevant regulations. The occurrence of AEs was calculated by the number of subjects who experienced at least one AE dividing the total number of subjects.

2.4. Measurement of Radioactivity

Plasma, urine, bile and cage rinse were directly analyzed for total radioactivity by liquid scintillation counting (LSC). Fecal samples were homogenized with isopropanol/water (50/50, v/v). Duplicate aliquots (0.3g) of each fecal homogenate were placed into combustion boats and burnt completely. The resulting $^{14}CO_2$ trapped was analyzed by LSC.

2.5. Metabolite Profiling and Identification

Plasma samples collected at each time point were pooled using the trapezoidal AUC pooling method [14], to obtain one representative plasma sample for male rats, one for female rats and one for male human volunteers. Moreover, plasma samples from individual animals or human volunteers were pooled at an equal volume, to obtain the following samples for each time point: one sample for male rats, one for female rats and one for male human volunteers. The samples of bile, urine or fecal homogenates were pooled across collection intervals at an equal percentage of collection volume to obtain one pooled sample for each individual. In addition, the excreta samples from rats or humans were pooled across individuals at an equal volume to get one pooled sample per time point for each specimen. The [^{14}C] labeled components were extracted from plasma and fecal homogenates by protein-precipitation with methanol, and the extracts were concentrated prior to analysis. Bile and urine samples were centrifuged prior to analysis. The samples of plasma, urine, feces, bile obtained above were injected to an HPLC system for fractionation, and then the radioactivity in each fraction was measured by solid scintillation counting using a Packard TopCount® NXT™ Microplate Counter. The radioactivity profiles were reconstructed using ARC® Convert and Evaluation software and the peak area of each radioactivity

peak/region was integrated to determine the percent distribution of individual radioactivity peaks or regions in each sample. The metabolite identification was carried out by liquid chromatography coupled to mass spectrometry in connection with radioactivity monitoring.

The HPLC system Shimadzu UFLC CBM-20A was used for fractionation and on-line detection. The separation was performed on a column of ACE 3 C18-AR (3.0 μm, 150 mm x 4.6 mm) at ambient temperature. The mobile phase consisted of 0.1 M ammonium acetate adjusted to pH 5.5 with acetic acid (A) and acetonitrile (B). The flow rate was 0.7 mL/min. The gradient elution started with 100% A for the first 3 minutes and then was executed as follows: linear increase of B from 0 to 20% in 12 minutes and remaining for 15 minutes, increase of B to 30% in 7 minutes and remaining for 10 minutes, increase of B to 50% in 13 minutes and then to 100% in 5 minutes, remaining 100% B for 5 minutes, and finally decrease of B to 0 in 2 minutes and remaining for 15 minutes. For better chromatographic separation between surufatinib and the metabolite M18, the HPLC conditions were optimized by setting the column temperature at 30°C and changing the mobile phase A to 0.4% formic acid (adjusted to pH 3.2 with ammonia). The gradient elution was executed as follows: 100% A for the first 2 minutes, increase of B from 0 to 30% in 1 minute and remaining for 10 minutes, increase of B to 40% in 5 minutes and remaining for 10 minutes, increase of B to 100% in 5 minutes and remaining for 5 minutes, and finally decrease of B to 0 in 2 minutes and remaining for 16 minutes. The mass spectrometry was conducted at the positive ion mode by LTQ-OrbiTrap XL or at the negative ion model by API-4000 QTrap. The instrument parameters (voltage, gas flow rates, temperature, collision energy, *etc.*) were optimized for maximal sensitivity of the analyte of interest.

2.6. *In vitro* Evaluations of Absorption and Metabolism

The Caco-2 permeability of surufatinib was evaluated. Caco-2 cells (purchased from Shanghai Institutes for Biological Sciences, Shanghai, China) were cultured in 24-well Transwell plates for 21 days to form monolayers. Surufatinib was added to either the apical (A) or the basolateral (B) side at 10 μM and incubated for 60 min. The samples on both sides were collected, and the concentration of surufatinib was determined. The apparent permeability coefficient (P_{app}) was calculated as follows: $P_{app}=\frac{Vr\times C_{r,t}}{S\times t\times C_{d,0}}$, where Vr, $C_{r,t}$, S, t and $C_{d,0}$ represent the volume of receive chamber, concentration in receiver chamber, surface area of the cell monolayer, incubation time and original concentration in donor chamber, respectively.

The metabolic stability of surufatinib was assessed in liver microsomes (purchased from BD Bioscience, New Jersey, US). Surufatinib (1 μM) was incubated with 0.5 mg/mL rat or human liver microsomes for up to 120 min. The incubation samples were collected at each time point, and the concentration of surufatinib was determined. The systemic clearance was estimated using the well-stirred model as follows: $CL_{sys} = CL_{int} \times Q_H/(Q_H + CL_{int})$, where CL_{int} and Q_H are estimated intrinsic clearance and hepatic blood flow, respectively.

The drug-metabolizing enzyme identification was conducted using liver microsomes and recombinant enzymes (purchased from CYPEX, Dundee, UK). Surufatinib (0.2 μM) was incubated with human liver microsomes for up to 120 min in the absence or presence of the specific inhibitor for each cytochrome P450 (CYP) enzyme (*i.e.*, α-naphthoflavone for CYP1A2, sulfaphenazole for CYP2C9, quinidine for CYP2D6 and ketoconazole for CYP3A4/5). The incubation samples were collected at each time point, and the concentration of surufatinib was determined. The CL_{int} of surufatinib was estimated in the absence or presence of the inhibitor for each CYP. The contribution of each CYP on surufatinib metabolism was assessed as follows: Contribution% =$(1-CL_{int,[I]}/CL_{int})\times 100\%$, where $CL_{int,[I]}$ is the CL_{int} in the presence of each inhibitor. The contribution of each CYP was subsequently evaluated using the recombinant human CYP enzymes (CYP3A4, CYP3A5, CYP2C8, CYP2C9, CYP2C19, CYP1A2, CYP2B6 and CYP2D6).

The concentration of surufatinib in the above samples was determined using a system consisting of an API4000 triple quadrupole mass spectrometer and a Shimadzu UPLC system (LC-30AD pump, SIL-30ACMP autosampler). Chromatographic separation was performed on a Waters Symmetry C_{18} (5 μm, 2.1×50 mm) column. Mobile phase A was water containing 0.1% formic acid, and mobile phase B was acetonitrile with 0.1% formic acid. The gradient elution was conducted as follows: mobile phase B: 5%-90% at 0-3.59 min, 90%-5% at 3.59-3.60 min, then 5% held during 3.60-5.00 min for re-equilibration before the next injection. The HPLC flow rate was set at 0.5 mL/min. Electrospray Ionization (ESI) source (positive mode) and multiple-reaction monitoring (MRM) mode were applied for the sample analysis.

2.7. Pharmacokinetic Analysis

The non-compartmental analysis was performed to obtain the pharmacokinetic parameters of the total radioactivity in plasma using WinNonlin (Version 7.0, Pharsight Corp.). The parameters included maximum observed concentration (C_{max}), time to C_{max} (T_{max}), area under the plasma concentration-time curve from time zero to the last measurable time point (AUC_{0-t}), area under the plasma concentration-time curve extrapolated to infinity ($AUC_{0-\infty}$), and the terminal half-life ($t_{1/2}$).

3. RESULTS

3.1. Pharmacokinetics in Rats and Humans

Following a single oral dose of [^{14}C] surufatinib, the total surufatinib derived radioactivity in plasma reached the peak (C_{max}) of 2103, 3229 and 405 ng Eq./g in male rats, female rats and male human volunteers, respectively, with the time to C_{max} (T_{max}) of 4 hours post-dose (Fig. **1**, Table **1**). Higher radioactivity exposure was observed in female rats than that in male rats. The elimination half-life ($t_{1/2}$) of the total radioactivity was markedly longer in humans than in rats.

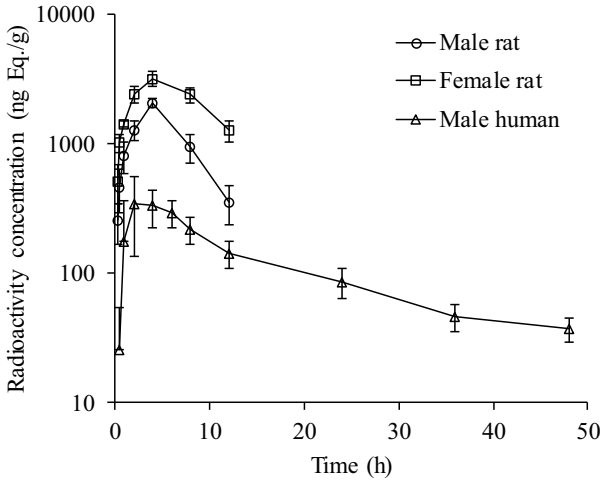

Fig. (1). Profiles of radioactivity concentration in plasma vs. time for rats and human volunteers following a single oral dose of [^{14}C] surufatinib (rat: 40 mg/kg; human: 300 mg).

3.2. Excretion in Rats and Humans

Following a single oral dose of [^{14}C] surufatinib in male rats, female rats and male human volunteers, the excretion of surufatinib-derived radioactivity is illustrated in Fig. (**2**).

Table 1. Pharmacokinetic parameters (mean ± SD) based on surufatinib-derived radioactivity in plasma following a single oral dose of 40 mg/100 μCi/kg [^{14}C] surufatinib in rats or 300 mg (100 μCi) in human volunteers.

Parameters	-	Male Rats (n=3)	Female Rats (n=3)	Male Humans (n=6)
T_{max}*	(h)	4 (4, 4)	4 (4, 4)	4 (2, 6)
C_{max}	(ng Eq./g)	2103±168	3229±448	405±184
$AUC_{0\text{-}12h}$	(h·ng Eq. /g)	13585±1261	27133±2471	5752±1732^
$AUC_{0\text{-}\infty}$	(h·ng Eq. /g)	15250±1890	39639±6729	6976±2090
$t_{1/2}$	(h)	3.12±0.517	6.48±2.48	23.3±6.68

*: median (min, max); ^: $AUC_{0\text{-}48h}$ except for $AUC_{0\text{-}72h}$ for one subject.

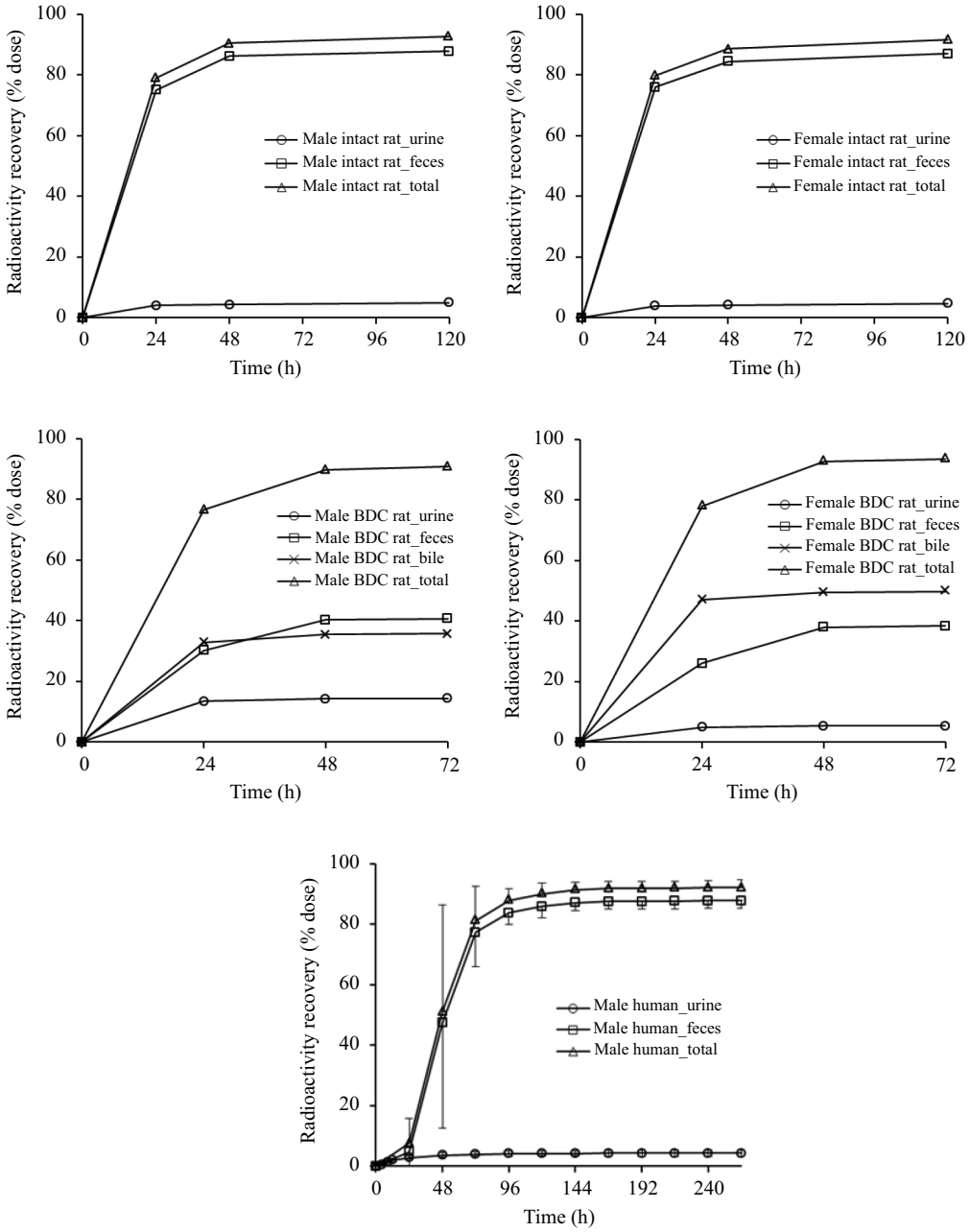

Fig. (2). Recovery of radioactivity in intact rats, bile duct cannulated (BDC) rats and human volunteers following a single oral dose of [^{14}C] surufatinib (rat: 40 mg/kg; human: 300 mg).

For intact rats, the total recovery of the radioactivity up to 120 hours post-dose was 93.4% and 92.5% in males and females, respectively. Urinary excretion accounted for 5.03% and 4.68% in males and females, respectively, and fecal excretion accounted for 87.8% and 87.0% in males and females, respectively. The majority of the radioactivity was recovered within 24 hours post-dose (79.4% and 80.4% in male and females, respectively), and nearly the total radioactivity (about 90%) was excreted within 48 hours post-dose. In BDC rats, the total recovery of the radioactivity up to 72 hours post-dose was 91.7% and 94.0% in males and females, respectively. Of the total, 35.8% was excreted in bile, 14.4% in urine and 40.7% in feces for males, and 49.8%, 5.40% and 38.5% for females.

In male human volunteers, the total recovery was 92.1% up to 264 hours post-dose, and 90.1% of the dose was recovered within 120 hours post-dose. Urinary excretion accounted for 4.29% of the dose, and fecal excretion for 87.9%.

3.3. Metabolism in Rats and Humans

Representative radio-chromatograms of plasma, urine and feces from rats and human volunteers and of rat bile are shown in Fig. (**3**). A further optimized LC method was used for the chromatographic separation between surufatinib and M18 (HM5013621). Characterization of surufatinib and its metabolites in rats and human volunteers is presented in Table **2**. The proposed metabolic pathway is shown in Fig. (**4**). Basically, the structures of metabolites were proposed based on the exact mass from the high-resolution mass spectrum for each molecular ion and then the ion fragmentations from product ion scan spectra. The high-resolution mass spectrum of surufatinib indicated the exact mass of 481.2008

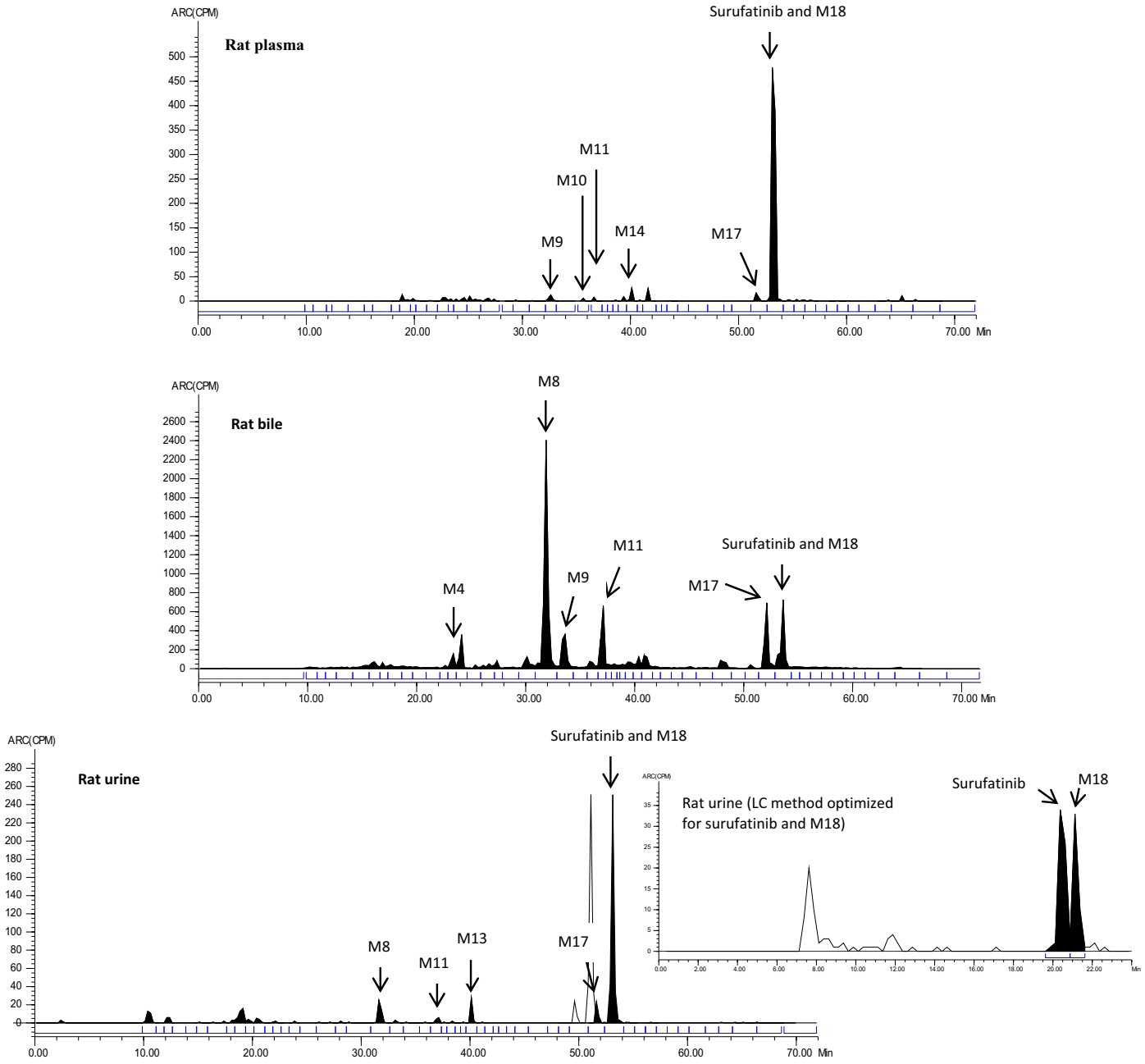

Fig. (3) contd…

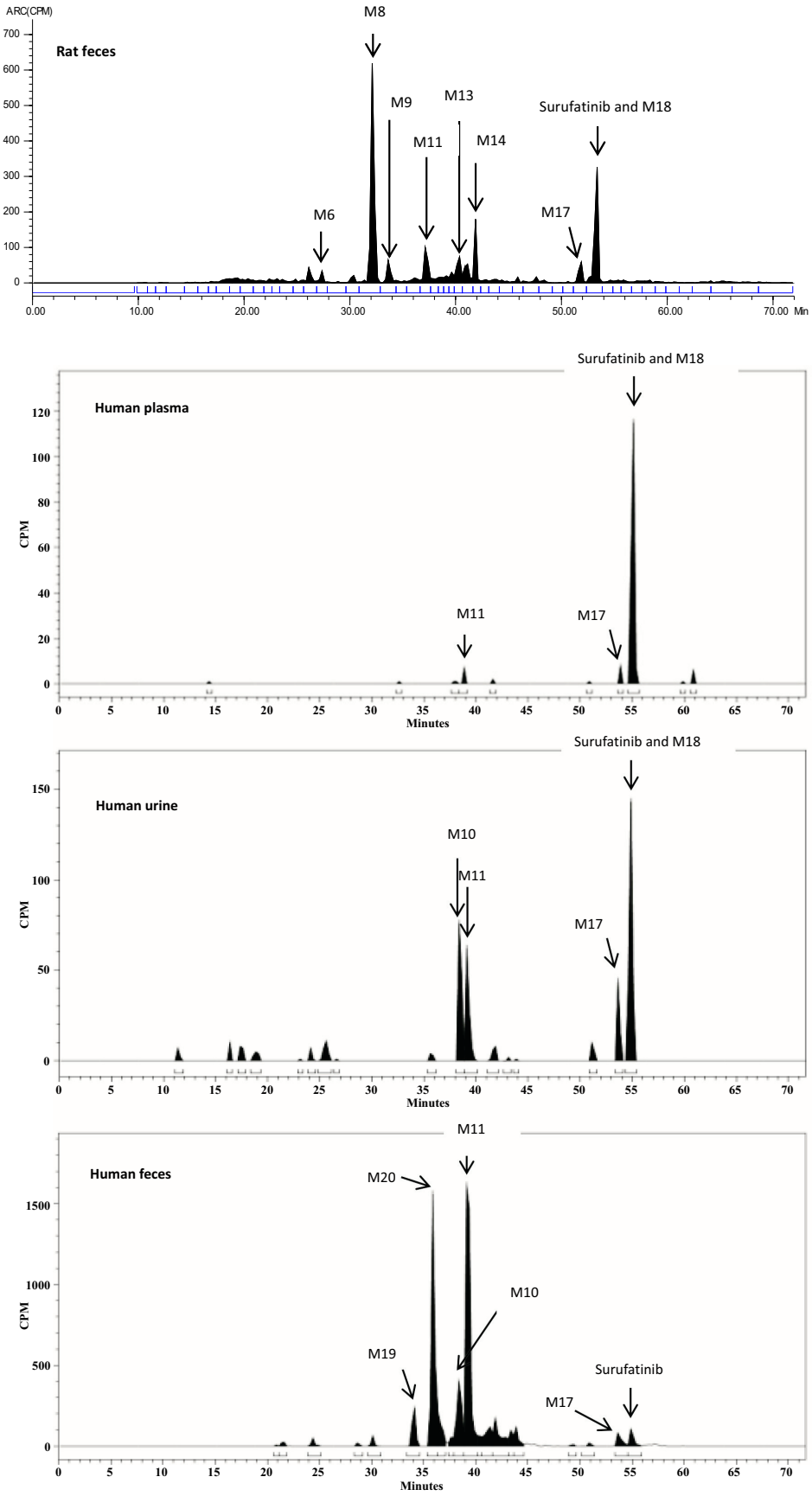

Fig. (3). Representative radio-chromatograms of plasma, urine, feces and bile (rat only) from rats and human volunteers.

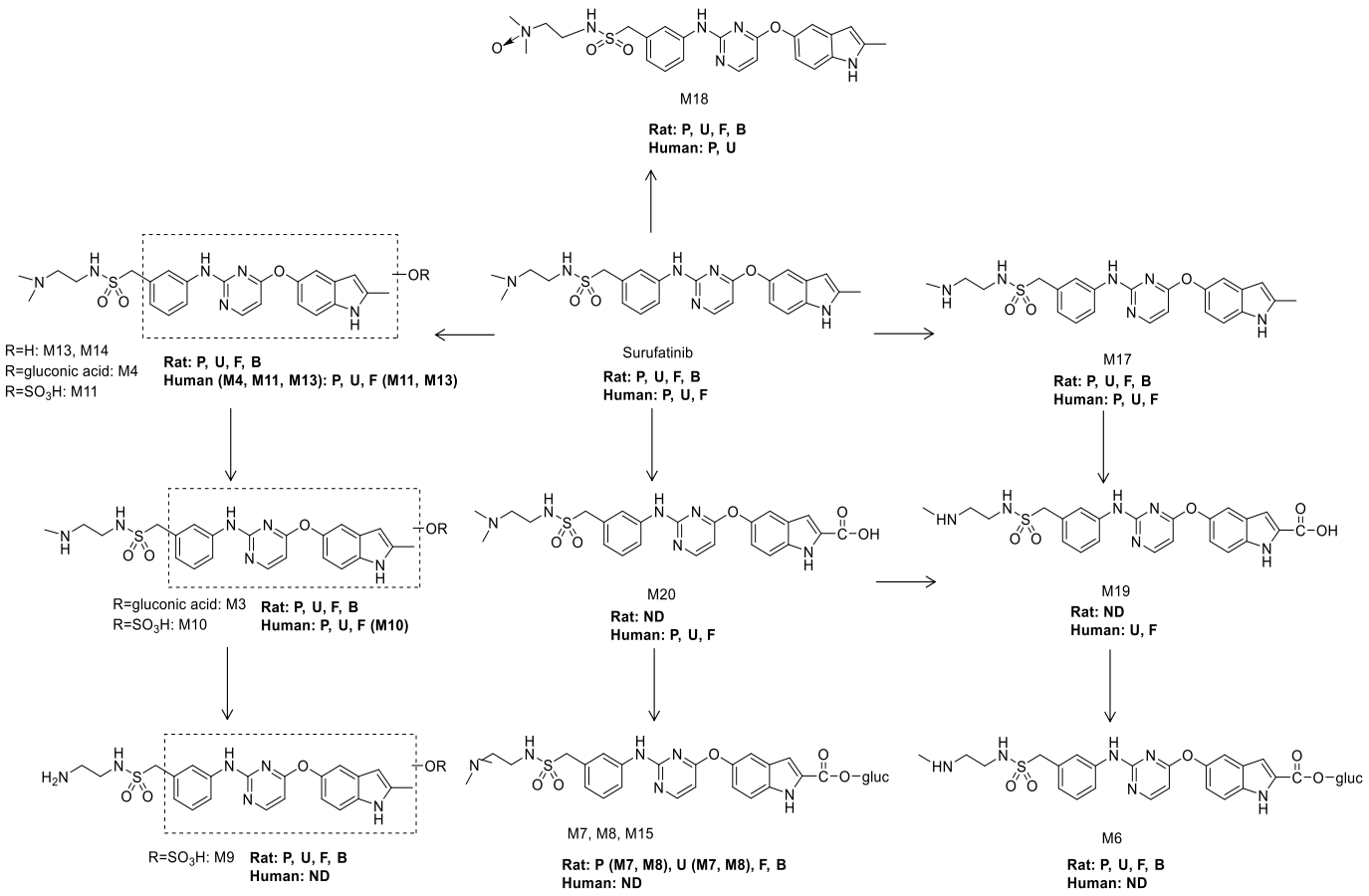

Fig. (4). The proposed metabolic pathway for surufatinib in rats and humans (P: plasma; U: urine; F: feces; B: bile; ND: not detected).

Table 2. Characterization of surufatinib and its metabolites in rats and human volunteers.

Metabolite	Structural Modification	Molecular ion ($[M+H]^+$)/Error (ppm)	Major Fragment Ions	Species/Matrix	
-	-	-	-	Rat	Human
Surufatinib	Parent	481.2008/-1.66	393, 347, 329	P, U, F, B	P, U, F
M3	N-demethylation, mono-oxidation, glucuronidation	659.2119/-1.67	483→345	P, U, F, B	P, U
M4	Mono-oxidation, glucuronidation	673.2280/-0.89	497→479, 345	P, U, F, B	P, U
M6	Carboxylation, N-demethylation, glucuronidation	673.1941/-1.88	497→359	P, U, F, B	ND
M7	Carboxylation, glucuronidation	687.2089/1.47	511→467, 377, 359	P, U, F, B	ND
M8	Carboxylation, glucuronidation	687.2087/1.21	511→467, 377, 359	P, U, F, B	ND
M9	N, N-didemethylation, mono-oxidation, sulfation	549.1230/1.75	469→405, 345	P, U, F, B	ND
M10	N-demethylation, mono-oxidation, sulfation	563.1388/1.95	483→363, 345	P, U, F, B	P, U, F
M11	Mono-oxidation, sulfation	577.1546/2.17	497→479, 363, 345	P, U, F, B	P, U, F
M13	Mono-oxidation	497.1987/4.29	479, 409, 345	P, U, F, B	P, U, F
M14	Mono-oxidation	497.1989/4.72	479, 363, 345	P, U, F, B	ND
M15	Carboxylation, glucuronidation	687.2114/5.02	511→467	B, F	ND
M17	N-demethylation	467.1867/1.44	347, 329	P, U, F, B	P, U, F
M18	Mono-oxidation	497.1973/1.50	436, 363, 345	P, U, F, B	P, U
M19	Carboxylation, N-demethylation	497.1601/-0.20	453, 377, 359	ND	U, F
M20	Carboxylation	511.1761/0.59	467, 377, 359	ND	P, U, F

P: plasma; U: urine; F: feces; B: bile; ND: not detected.

Table 3. Percentage of each surufatinib-derived radioactivity accounting for the total radioactivity in plasma (%AUC) following a single oral dose of 40 mg/100 μCi/kg [^{14}C] surufatinib in rats or 300 mg (100 μCi) in human volunteers.

Metabolite	Male Rats		Female Rats		Male Humans	
-	$AUC_{0\text{-}24h}$ (ng Eq·h/g)	%AUC	$AUC_{0\text{-}24h}$ (ng Eq·h/g)	%AUC	$AUC_{0\text{-}48h}$ (ng Eq·h/g)	%AUC
Total radioactivity	16929	100	33513	100	5750	100
Surufatinib	4393	25.9	16754	50.0	2310	40.2
M3	639	3.77	39.1	0.12	+	-
M4	ND	-	302	0.90	+	-
M6	639	3.77	302	0.90	ND	-
M7	ND	-	39.1	0.12	ND	-
M8	ND	-	20.6	0.06	ND	-
M9	639	3.77	424	1.26	ND	-
M10	718	4.24	120	0.36	+	-
M11	718	4.24	161	0.48	22.7	0.39
M13	359	2.12	603	1.80	+	-
M14	877	5.18	544	1.62	ND	-
M15	ND	-	ND	ND	ND	-
M17	159	0.94	484	1.44	205	3.57
M18	194	1.15	1039	3.10	385	6.70
M19	ND	-	ND	ND	ND	-
M20	ND	-	ND	ND	+	-

ND: not detected; +: detected only by LC-MS/MS.

Based on the radioactivity exposure ($AUC_{0\text{-}24h}$ for rats and $AUC_{0\text{-}48h}$ for humans), unchanged surufatinib was the major component in the plasma extract, accounting for 25.9%, 50.0% and 40.2% of the total radioactivity in plasma for male rats, female rats and male human volunteers, respectively. The exposure percentage (%AUC) of the parent drug in plasma was lower in male rats than that in female rats, and higher %AUC was observed for metabolites in male rats than that in female rats (Table **3**). The circulating metabolite with %AUC >3% in male rat plasma was M3 (N-demethylation+mono-oxidation+glucuronidation), M6 (carboxy-lation+N-demethylation+glucuronidation), M9 (N, N-didemethy-lation+mono-oxidation+sulfation), M10 (N-demethylation+mono-oxidation+sulfation), M11 (mono-oxidation+sulfation) and M14 (mono-oxidation). The metabolites above were detected at much lower levels in female rat plasma. For the other metabolites M13 (mono-oxidation), M17 (N-demethylation) and M18 (mono-oxidation at the tertiary amine, HM5013621) detected in male rat plasma, the %AUC of each was <3% and similar to that in female plasma. The number of metabolites detected in human plasma was not as many as that in rat plasma. The two major metabolites in human plasma were M17 and M18, and %AUC was 3.57% and 6.70%, respectively. The radioactivity exposure to the parent drug and the metabolites approximately accounted for 60% of the total exposure in rat plasma and 50% in human plasma. About 40% of the total radioactivity in rat plasma and about 50% in human plasma were measured in the post-extraction pellets of plasma samples.

The percentage of each surufatinib related radioactive component in excreta accounting for the dose (%dose) is listed in Table **4**. In intact rats, the parent drug in urine accounted for 0.81% of the dose for males and 0.98% for females, within 120 hours post-dose. The levels of metabolites in urine were lower or much lower than the parent exposure (except for 1.73% for M18 in female urine). The parent drug in feces accounted for 6.98% for males and 8.52% for females. The most abundant metabolite in feces was M8 (carboxylation+glucuronidation), accounting for 14.5% for males and 16.0% for females. The values of %dose for each metabolite detected in feces were similar between males and females. In addition to M8, the metabolites in rat feces with %dose > 3% were M11, M14 and M17 (1.74% for females). In BDC rats, the most abundant radioactive component in bile was M8, with the %dose of 9.46% for males and 15.1% for females up to 72 hours post-dose, which was similar to the finding in feces. The parent drug excreted in bile accounted for 1.43% of the dose for males and 3.48% for females, and M11 and M17 were the metabolites detected in bile with the levels of close to or slightly higher than 3% of the dose. For human volunteers, M11 and M20 (carboxylation) were the most abundant radioactive components in excreta (mainly detected in feces), and the radioactivity in feces was 19.9% and 18.6% of the dose, respectively. The parent drug in urine and feces accounted for 1.37% and 3.25% of the dose, respectively. The radioactivity of the parent drug and the metabolites in feces accounted for about 40% of the dose for both rats and human volunteers, and the radioactivity measured in the post-extraction pellets of feces samples was about 30% for rats and about 20% for humans, respectively.

3.4. Safety in Humans

Four out of six volunteers experienced at least one AE in this study. The reported AEs were sinus bradycardia (4, 66.7%), sinus arrhythmia (1, 16.7%), and hyperuricemia (1, 16.7%) with Grade 1. No clinically relevant findings were observed in physical

Table 4. Excretion (%dose) of surufatinib and metabolites following a single oral dose of 40 mg/100 μCi/kg [^{14}C] surufatinib in rats or 300 mg (100 μCi) in human volunteers.

Metabolite	Intact Rats (% Dose)						BDC Rats (% Dose)		Humans (% Dose)		
-	Male	-	-	Female	-	-	Male	Female	Male	-	-
-	Urine (0-120 h)	Feces (0-120 h)	Total	Urine (0-120 h)	Feces (0-120 h)	Total	Bile (0-72 h)	Bile (0-72 h)	Urine (0-264 h)	Feces (0-264 h)	Total
Surufatinib	0.81	6.98	7.79	0.98	8.52	9.50	1.43	3.48	1.37	3.25	4.62
M3	0.02	0.40	0.42	ND	0.37	0.37	0.30	0.21	+	ND	-
M4	0.02	0.30	0.32	0.02	0.44	0.46	0.51	0.97	+	ND	-
M6	<0.01	0.98	0.98	0.02	0.84	0.86	0.15	0.44	ND	ND	-
M7	<0.01	1.51	1.51	<0.01	0.73	0.73	2.23	1.20	ND	ND	-
M8	0.29	14.5	14.8	0.33	16.0	16.33	9.46	15.1	ND	ND	-
M9	0.05	1.88	1.93	0.03	1.90	1.93	1.12	3.18	ND	ND	-
M10	0.04	1.05	1.09	<0.01	0.78	0.78	2.60	0.75	0.73	5.77	6.50
M11	0.17	3.05	3.22	0.08	3.11	3.19	2.86	3.84	0.71	19.9	20.6
M13	0.29	1.78	2.07	0.24	2.43	2.67	0.58	0.69	+	+	-
M14	0.02	4.63	4.65	ND	3.35	3.35	0.89	1.24	ND	ND	-
M15	ND	0.83	0.83	ND	0.32	0.32	1.48	1.02	ND	ND	-
M17	0.58	3.11	3.69	0.25	1.74	1.99	2.85	4.18	0.56	4.06	4.62
M18	0.58	0.28	0.86	1.73	0.34	2.07	1.74	0.99	0.27	ND	0.27
M19	ND	ND	-	ND	ND	-	ND	ND	+	4.26	4.26
M20	ND	ND	-	ND	ND	-	ND	ND	+	18.6	18.6

ND: not detected; +: detected only by LC-MS/MS.

examination, vital signs measurements, and no serious adverse events occurred.

3.5. *In vitro* Evaluations of Absorption and Metabolism

The Caco-2 permeability study showed that the apparent permeability coefficient ($P_{app, A-B}$) of surufatinib was 4.1×10^{-6} cm/s. Based on the data of metabolic stability in liver microsomes, CL_{sys} was estimated to be 54.8 mL/min/kg for rat and 15.7 mL/min/kg for humans. In the enzyme phenotyping study, surufatinib was barely metabolized in human liver microsomes unless NADPH was added to the incubation system, which indicated that CYPs played a major role in the metabolism of surufatinib. The subsequent studies in the liver microsomes with CYP inhibitors and in the recombinant human CYPs showed that CYP3A4 was the predominant enzyme mediating surufatinib metabolism with the contribution% > 85%.

4. DISCUSSION

The pharmacokinetics, metabolism and excretion of surufatinib were investigated in rats and humans following a single oral dose of [^{14}C] surufatinib. Surufatinib was orally absorbed similarly in rats and humans, with the median T_{max} of 4 hours post-dose. The radioactivity exposure in plasma was higher in female rats than in males. Only males were enrolled in the human study. The previous population pharmacokinetic analysis internally conducted on the data of patients (110 males and 81 females) indicated that gender was not a significant covariate on surufatinib pharmacokinetics in humans (median of oral clearance CL/F: 18.5 mL/min/kg for male and 15.5 mL/min/kg for female). The estimated $t_{1/2}$ appeared shorter in rats than in humans, which was partially due to the elimination phase of the concentration-time profile for rats constructed not as sufficiently as done for humans. For rats, the radioactivity in plasma decreased to lower than 137 ng Eq./g (lower limit of quantification, LLOQ) after 12 hours post-dose. When determining the radioactivity in the human plasma samples, the volume of plasma was increased to 1 g from 0.05 g previously used in the rat study, and the samples up to 48 hours post-dose were detected with measurable radioactivity (>30.3 =(1-$CL_{int\ ,[I]}$ Eq./g). The study of *in vitro* metabolic stability in liver microsomes predicted that the systemic clearance of surufatinib was high and close to the hepatic blood flow of respective species (55 mL/min/kg for rat and 21 mL/min/kg for human), which may also help to explain the observed difference of *in vivo* elimination between rats and humans from the physiological perspective, *i.e.* the higher hepatic blood flow led to the more rapid elimination of surufatinib in rats than in humans. The *in vitro* Caco-2 permeability data indicated a moderate transport rate for surufatinib. The high clearance and the moderate transport rate hampered a high oral bioavailability, and the absolute bioavailability of surufatinib has yet to be evaluated in humans.

Following a single oral dose, the excretion of surufatinib was almost complete in rats and human volunteers in the studies, with the total radioactivity recovery of >90% of the dose. Similarly, in rats and humans, fecal excretion predominated as indicated by approximately 87% of the dose recovered in feces and only 5% in

urine. No sex difference in radioactivity excretion was observed in rats. The radioactivity was excreted more slowly in humans than in rats, *i.e.*, 120 hours in humans versus 48 hours in rats spent on 90% of the dose recovered. According to the excretion data for BDC rats, nearly half of the radioactivity eventually discharged in feces came from the bile secretion, indicating the important role of hepatic extraction in the elimination of surufatinib.

The parent drug, surufatinib, was the major radioactive component detected in the plasma extracts of rats and humans, and there was not a single circulating metabolite accounting for >10% of the total radioactivity. The levels of circulating metabolites were higher in male rats than in females. The major circulating metabolite in humans was M18 (mono-oxidation at the tertiary amine, HM5013621), which was also detected in rats. Similarly, in rats and humans, about 50% of the radioactivity was measured in the post-extraction pellets of plasma. It was speculated that certain reactive metabolites were formed and then covalent-bond to plasma proteins. The acyl glucuronide metabolites of surufatinib, *i.e.*, M6, M7, M8 and M15, were the suspected species that contributed to the covalent binding [15]. Toxicology studies have been carried out in rats, which was considered providing the toxicity evaluation on the covalent binding in the preclinical settings. The *in vitro* enzyme phenotyping study indicated that CYP3A4 was the major enzyme mediating surufatinib metabolism.

Following a single oral dose, fecal excretion was the predominant way for the elimination of surufatinib and its metabolites in rats and humans. The recovery of surufatinib in the form of parent drug was minor in the excreta (<10% of the dose for rat and <5% for humans, and mainly excreted in feces). The most abundant metabolite in rat feces was M8 (carboxylation+glucuronidation), which obviously came from biliary secretion as shown by the data of BDC rats. The two most abundant metabolites in human's feces were M11 (mono-oxidation+sulfation) and M20 (carboxylation), each similarly accounting for approximately 20% of the dose. M11 was also detected in rat feces. For M20, it was thought that it is the hydrolysis product of glucuronides M7, M8 or M15, and the hydrolysis occurred in the intestine after the glucuronides were discharged *via* bile. It was observed that for the carboxylation metabolite M20 its conjugates of glucuronic acid existed in rat feces but mainly in the form of aglycone in human feces. This difference in fecal excretion between rats and humans was also observed for M19 (carboxylation+N-demethylation) and its conjugate of glucuronic acid (M6). The removal of glucuronic acid from glucuronides may be attributed to gut bacterial β-glucuronidases [16, 17], and the difference between rat and human has yet to be studied.

CONCLUSION

Following oral administration, fecal excretion was predominant in the elimination of surufatinib in rats and humans, and biliary secretion markedly contributed to the fecal excretion. No disproportionate circulating metabolite was observed in humans.

ETHICS APPROVAL AND CONSENT TO PARTICIPATE

The study protocol for mice was approved by XBL-China's Institutional Animal Care and Use Committee (IACUC), Nanjing, China.

HUMAN AND ANIMAL RIGHTS

No humans were used for this study. The protocol for the rat AME study was reviewed and approved by XBL-China's Institutional Animal Care and Use Committee (IACUC). The protocol for the human AME study was reviewed and approved by the ethical committee at the First Affiliated Hospital of Soochow University, Suzhou, China.

CONSENT FOR PUBLICATION

Not applicable.

AVAILABILITY OF DATA AND MATERIALS

Not applicable.

FUNDING

This work was sponsored and funded by Hutchison MediPharma Ltd. and supported by the National Key New Drug Creation Special Programs (No. 2017ZX09304021), Jiangsu Provincial Medical Youth Talent (No. QNRC2016714), National Natural Science Foundation of China (No. 81773820), the Jiangsu Provincial Medical Talent (No. ZDRCA2016048) and the Suzhou Key Laboratory of Drug Clinical Research and Personalized Medicine (No. SZS201719).

CONFLICT OF INTEREST

Ke Li, Songhua Fan, Bin Pan, Weihan Zhang and Weiguo Su are the employees of Hutchison MediPharma Ltd. (the sponsor of the studies).

ACKNOWLEDGEMENTS

Declared none.

REFERENCES

[1] Dasari, A.; Shen, C.; Halperin, D.; Zhao, B.; Zhou, S.; Xu, Y.; Shih, T.; Yao, J.C. Trends in the incidence, prevalence, and survival outcomes in patients with neuroendocrine tumors in the United States. *JAMA Oncol.,* **2017**, *3*(10), 1335-1342. http://dx.doi.org/10.1001/jamaoncol.2017.0589 PMID: 28448665

[2] Fan, J.H.; Zhang, Y.Q.; Shi, S.S.; Chen, Y.J.; Yuan, X.H.; Jiang, L.M.; Wang, S.M.; Ma, L.; He, Y.T.; Feng, C.Y.; Sun, X.B.; Liu, Q.; Deloso, K.; Chi, Y.; Qiao, Y.L. A nation-wide retrospective epidemiological study of gastroenteropancreatic neuroendocrine neoplasms in china. *Oncotarget,* **2017**, *8*(42), 71699-71708. http://dx.doi.org/10.18632/oncotarget.17599 PMID: 29069739

[3] Pavel, M.; O'Toole, D.; Costa, F.; Capdevila, J.; Gross, D.; Kianmanesh, R.; Krenning, E.; Knigge, U.; Salazar, R.; Pape, U.F.; Öberg, K. Vienna Consensus Conference participants. Vienna Consensus Conference participants. ENETS consensus guidelines update for the management of distant metastatic disease of intestinal, pancreatic, bronchial neuroendocrine neoplasms (NEN) and NEN of unknown primary site. *Neuroendocrinology,* **2016**, *103*(2), 172-185. http://dx.doi.org/10.1159/000443167 PMID: 26731013

[4] Phan, A.T.; Halperin, D.M.; Chan, J.A.; Fogelman, D.R.; Hess, K.R.; Malinowski, P.; Regan, E.; Ng, C.S.; Yao, J.C.; Kulke, M.H. Pazopanib and depot octreotide in advanced, well-differentiated neuroendocrine tumours: a multicentre, single-group, phase 2 study. *Lancet Oncol.,* **2015**, *16*(6), 695-703. http://dx.doi.org/10.1016/S1470-2045(15)70136-1 PMID: 25956795

[5] Raymond, E.; Dahan, L.; Raoul, J.L.; Bang, Y.J.; Borbath, I.; Lombard-Bohas, C.; Valle, J.; Metrakos, P.; Smith, D.; Vinik, A.; Chen, J.S.; Hörsch, D.; Hammel, P.; Wiedenmann, B.; Van Cutsem, E.; Patyna, S.; Lu, D.R.; Blanckmeister, C.; Chao, R.; Ruszniewski, P. Sunitinib malate for the treatment of pancreatic neuroendocrine tumors. *N. Engl. J. Med.,* **2011**, *364*(6), 501-513. http://dx.doi.org/10.1056/NEJMoa1003825 PMID: 21306237

[6] Kulke, M.H.; Lenz, H.J.; Meropol, N.J.; Posey, J.; Ryan, D.P.; Picus, J.; Bergsland, E.; Stuart, K.; Tye, L.; Huang, X.; Li, J.Z.; Baum, C.M.; Fuchs, C.S. Activity of sunitinib in patients with advanced neuroendocrine tumors. *J. Clin. Oncol.,* **2008**, *26*(20), 3403-3410. http://dx.doi.org/10.1200/JCO.2007.15.9020 PMID: 18612155

[7] Tran, T.A.; Leong, H.S.; Pavia-Jimenez, A.; Fedyshyn, S.; Yang, J.; Kucejova, B.; Sivanand, S.; Spence, P.; Xie, X.J.; Peña-Llopis, S.; Power, N.; Brugarolas, J. Fibroblast growth factor receptor-dependent and -independent paracrine signaling by sunitinib-resistant renal cell carcinoma. *Mol. Cell. Biol.,* **2016**, *36*(13), 1836-1855. http://dx.doi.org/10.1128/MCB.00189-16 PMID: 27141054

[8] Ries, C.H.; Cannarile, M.A.; Hoves, S.; Benz, J.; Wartha, K.; Runza, V.; Rey-Giraud, F.; Pradel, L.P.; Feuerhake, F.; Klaman, I.; Jones, T.; Jucknischke, U.; Scheiblich, S.; Kaluza, K.; Gorr, I.H.; Walz, A.; Abiraj, K.; Cassier, P.A.; Sica, A.; Gomez-Roca, C.; de Visser, K.E.; Italiano, A.; Le Tourneau, C.; Delord, J.P.; Levitsky, H.; Blay, J.Y.; Rüttinger, D. Targeting tumor-associated macrophages with anti-CSF-

1R antibody reveals a strategy for cancer therapy. *Cancer Cell,* **2014**, *25*(6), 846-859.
http://dx.doi.org/10.1016/j.ccr.2014.05.016 PMID: 24898549

[9] Xu, J.M.; Wang, Y.; Chen, Y.L.; Jia, R.; Li, J.; Gong, J.F.; Li, J.; Qi, C.; Hua, Y.; Tan, C.R.; Wang, J.; Li, K.; Sai, Y.; Zhou, F.; Ren, Y.X.; Qing, W.G.; Jia, H.; Su, W.G.; Shen, L. Sulfatinib, a novel kinase inhibitor, in patients with advanced solid tumors: results from a phase I study. *Oncotarget,* **2017**, *8*(26), 42076-42086.
http://dx.doi.org/10.18632/oncotarget.14942 PMID: 28159938

[10] Xu, J.; Li, J.; Bai, C.; Xu, N.; Zhou, Z.; Li, Z.; Zhou, C.; Jia, R.; Lu, M.; Cheng, Y.; Mao, C.; Wang, W.; Cheng, K.; Su, C.; Hua, Y.; Qi, C.; Li, J.; Wang, W.; Li, K.; Sun, Q.; Ren, Y.; Su, W. Surufatinib in advanced well-differentiated neuroendocrine tumors: a multicenter, single-arm, open-label, phase Ib/II trial. *Clin. Cancer Res.,* **2019**, *25*(12), 3486-3494.
http://dx.doi.org/10.1158/1078-0432.CCR-18-2994 PMID: 30833272

[11] U. S. Food and Drug Administration/Center for Drug Evaluation and Research. Guidance for industry: safety testing of drug metabolites. FDA: Silver Spring, **2020**. Available at: https://www.fda.gov/media/72279/download

[12] U. S. Food and Drug Administration/Center for Drug Evaluation and Research, Guidance for industry: pharmacokinetics in patients with impaired hepatic function: study design, data analysis, and impact on dosing and labeling. FDA: Rockville, **2003**. Available at: https://www.fda.gov/media/71311/download

[13] U. S. Food and Drug Administration/Center for Drug Evaluation and Research, Guidance for industry: clinical drug interaction studies - cytochrome P450 enzyme- and transporter-mediated drug interactions. FDA: Silver Spring,, **2020**. Available at: https://www.fda.gov/media/134581/download

[14] Hop, C.E.; Wang, Z.; Chen, Q.; Kwei, G. Plasma-pooling methods to increase throughput for *in vivo* pharmacokinetic screening. *J. Pharm. Sci.,* **1998**, *87*(7), 901-903.
http://dx.doi.org/10.1021/js970486q PMID: 9649361

[15] Van Vleet, T.R.; Liu, H.; Lee, A.; Blomme, E.A.G. Acyl glucuronide metabolites: Implications for drug safety assessment. *Toxicol. Lett.,* **2017**, *272*, 1-7.
http://dx.doi.org/10.1016/j.toxlet.2017.03.003 PMID: 28286018

[16] Biernat, K.A.; Pellock, S.J.; Bhatt, A.P.; Bivins, M.M.; Walton, W.G.; Tran, B.N.T.; Wei, L.; Snider, M.C.; Cesmat, A.P.; Tripathy, A.; Erie, D.A.; Redinbo, M.R. Structure, function, and inhibition of drug reactivating human gut microbial β-glucuronidases. *Sci. Rep.,* **2019**, *9*(1), 825-839.
http://dx.doi.org/10.1038/s41598-018-36069-w PMID: 30696850

[17] Collins, S.L.; Patterson, A.D. The gut microbiome: an orchestrator of xenobiotic metabolism. *Acta Pharm. Sin. B,* **2020**, *10*(1), 19-32.
http://dx.doi.org/10.1016/j.apsb.2019.12.001 PMID: 31998605